Reaction Kinetics, Mechanisms and Catalysis
https://doi.org/10.1007/s11144-024-02666-2

Study of the pyrolysis of polyester/viscose fibers catalyzed by tungsten-manganese bimetal supported montmorillonite

Pingli Li[1] · Qi Yang[3] · Hongmei Peng[2,3]

Received: 20 March 2024 / Accepted: 21 May 2024

Abstract

The upgrading of pyrolysis deoxygenation of polyester/viscose fibers was examined in this paper utilizing montmorillonite (MMT) catalysts with varying ratios and amounts of tungsten-manganese bimetallic. The temperature-programmed desorption of NH_3 (NH_3-TPD) revealed that after tungsten-manganese bimetal loading, MMT formed novel acidic sites, resulting in a considerable rise in total acidity. The maximum aromatics yield (73.10%) was achieved by the MMT with a bimetal loading of 10 wt%, the yield of monocyclic aromatic hydrocarbons (MAHs) was highest at 40.38%, while the yield of polycyclic aromatic hydrocarbons (PAHs) was lowest. The MAHs yield dramatically dropped at 15 wt% and 20 wt% bimetal loading. The application of a moderate load has the potential to facilitate the generation of MAHs, whilst an excessive load can readily facilitate the development of PAHs. The acid equilibrium of MMT was enhanced following the application of varying ratios of tungsten-manganese bimetal loading. When the ratio of bimetal load was 1:1, a significant synergistic impact was seen, resulting in a substantial enhancement of the catalyst regulation performance on MAHs and PAHs. Specifically, the catalyst exhibited a tendency to generate a higher proportion of useful MAHs (40.38%) while simultaneously reducing the production of PAHs (32.72%). This phenomenon can be attributed to the appropriate pore structure and the equitable distribution of Lewis acid and Brønsted acid sites within the pores.

Keywords Waste textiles · Polyester · Viscose · Catalytic fast pyrolysis · Bimetal

✉ Hongmei Peng
phm456@126.com

[1] Sichuan Fire Research Institute of MEM, Chengdu, China

[2] Chengdu Textile College, Chengdu, China

[3] College of Polymer Science and Engineering, The State Key Laboratory for Polymer Materials Engineering of Sichuan University, Chengdu, China

Published online: 27 May 2024

Introduction

The rise in demand for textiles has resulted in a corresponding increase in the production of textile waste. Unfortunately, the current absence of viable recycling methods has led to fewer than 1% of textile waste being effectively repurposed into fibers for the creation of new textile products. Consequently, the majority of waste textiles are either discarded in landfills or incinerated [1]. Theoretically, it is possible to recycle up to 95% of waste textiles. However, the actual recycling rates are far lower, with China achieving only 10–15%, the United States achieving 15.2%, and the European Union achieving 25% [2]. The primary factor contributing to the suboptimal recycling rate of waste textiles is the pressing necessity to address certain technical obstacles, including the development of efficient and expeditious fiber component identification and sorting technologies [3]. Textile waste is produced via the utilization of diverse forms and varieties of primary materials, including fibers, yarns, textiles, and garments, among others. Consequently, the generation of garbage exhibits significant disparities. Moreover, waste textiles consist of a variety of components, such as cellulose fibers and synthetic non-cellulose fibers, hence posing challenges in terms of their bioprocessing capabilities.

Recycling textile waste made of a single component is comparatively simple. For example, one potential application involves utilizing biobased textile waste as a substitute raw material for the synthesis of biological products via the bioconversion of the cellulose component of the textile. Following the bioconversion process, the cellulose portion is retained as a purified value-added product. However, the presence of numerous synthetic fibers and dyes within the fabric presents obstacles during the sorting procedure and diminishes the quality of the reclaimed material [4]. In the context of multi-component systems, certain textile waste remains non-recyclable due to its heterogeneous nature, comprising a combination of natural and synthetic fibers (e.g., cotton and polyester fabric blends) [5]. The retrieval of blends necessitates the depolymerization or dissolution of one or both constituents. For instance, the dissolution of polyester typically entails the use of hazardous solvents (such as DMSO) and elevated temperatures, which may have an impact on the characteristics of cellulose components. Cellulose degradation under acidic environments is facilitated by a comparable approach. An illustrative instance involves the utilization of hydrochloric acid to hydrolyze cotton, resulting in the production of microcrystalline cellulose powder. This powder can subsequently be separated from the residual polyester fabric, thereby enabling the recovery and subsequent reuse of the polyester material for the creation of novel textiles [6]. However, when considering the financial implications of recycling and the impact on the environment, the recovery and treatment of textile fibers pose significant challenges for multi-component systems.

The conversion of underutilized textile resources into energy presents a potential solution for addressing energy demands, waste treatment, and waste management. The integration of environmental factors, available resources, and energy sources can serve as a crucial catalyst in attaining objectives related to

environmental preservation, waste administration, and energy generation [7]. The process of upcycling involves the conversion of substances with low value into products of higher value through recycling [8, 9]. Thermochemical techniques possess the capability to effectively address a wide range of textile waste, exhibiting rapid reaction rates and facilitating substantial product throughput [10]. Pyrolysis stands out as a very efficient technique for managing diverse and intricate waste materials, making it a representative waste-to-energy approach. Due to the heterogeneous composition of textile waste, encompassing both synthetic and natural fibers, pyrolysis emerges as a highly promising avenue for the upgrading of textile waste in its life cycle. For instance, pyrolysis has shown to be highly effective for textile waste to recover renewable fuels such as cotton cellulose [11] and disposable masks [12]. Pyrolysis is therefore regarded as a potential upcycling technique for textile waste [13]. Catalytic pyrolysis is a process that enables the direct conversion of solid feedstocks into liquid fuels, commonly known as bio-oils, which exhibit a high degree of similarity to fuels generated from petroleum sources [14]. Catalytic fast pyrolysis (CFP) refers to the process of enhancing the quality of desired products, such as bio-oil, by employing catalysts prior to the rapid cooling of the pyrolysis volatiles. The implementation of upgraded technology enables the selective regulation of pyrolysis product distribution, resulting in an enhanced yield of desired products and consequently, an improved bio-oil quality. Throughout this procedure, a sequence of chemical events including pyrolysis, deoxygenation (specifically decarbonylation, decarboxylation, and dehydration), oligomerization, and aromatization may take place. These reactions serve to eliminate substantial quantities of oxygen from the initial material, resulting in the release of CO, CO_2, and H_2O [15, 16].

The catalyst is primarily composed of two primary components, namely the active substance and the support. The synergy between the two components has the potential to enhance the catalytic efficacy [17]. The development of appropriate catalysts plays a pivotal role in determining catalytic efficiency, product specificity, and durability when subjected to pyrolysis reaction conditions [18]. The catalyst's active and carrier catalysts work synergistically to modulate the interface between the active site and the pyrolysis steam, as well as the catalytic reaction pathway. This results in an enhanced selectivity of the desired product. The utilization of naturally plentiful minerals can offer cost-effective catalysts for the mild pyrolytic steam upgrading process. Montmorillonite (MMT), a type of solid acid clay catalyst, has demonstrated the ability to enhance the quality of bio-oils [19]. The utilization of metal-modified support has been demonstrated as a viable approach to enhance catalytic activity, mitigate catalyst deactivation resulting from coke deposition on the catalyst surface, and enhance the yield and selectivity of aromatics in the CFP process [20]. The introduction of a second active metal into a monometallic system can induce substantial modifications in both the electrical and geometric configuration of the catalyst. Consequently, the physical and chemical characteristics of the catalyst can exhibit notable disparities compared to those of the monometallic counterpart upon the incorporation of a second metal. Numerous studies have demonstrated that bimetallic catalysts manifest enhanced catalytic efficacy in diverse industrial applications when compared to their single metal counterparts. The utilization of

bimetal catalysts has been seen to yield a substantial enhancement in catalytic activity, thereby facilitating the process of thermal cracking of raw materials and the subsequent generation of aromatic hydrocarbons [21, 22]. The findings of Miskolczi et al. [23] demonstrated that the use of a Ni/Mo catalyst resulted in an augmentation of the rates of cracking, dehydrogenation, and decarboxylation processes. It is noteworthy to mention that the collective impact of bimetallic catalysts was not consistently significant. Specifically, the Zn/Ga multifunctional catalyst exhibited a reduced preference for aromatic hydrocarbons compared to the carrier catalyst. However, the simultaneous introduction of Co and Zn enhanced the catalytic performance of the carrier catalyst. Likewise, variations in metal loading ratios will exert an influence on the resultant product and its corresponding distribution. In their study, Balasundram et al. [24] employed a multifunctional catalyst that was synthesized with varying proportions of nickel (Ni) and cerium (Ce) to generate diverse yields of C_6-C_8 hydrocarbons during the catalytic pyrolysis of bagasse oil. In summary, the selection of appropriate metals for the catalyst surface can yield favorable outcomes, contingent upon the specific experimental subject.

Polyester fiber (PET), cotton fiber (CF), and viscose fiber (VF) are the predominant textile fibers in terms of usage. These three fibers, individually or in combination, are widely utilized in the production of textile textiles, thereby commanding a significant portion of the market. The recycling process of these three fibers has the potential to effectively address the recycling needs of a significant portion of textile waste. The utilization of natural fibers, such as cotton fibers, is hindered by the issue of land competition between grain and cotton crops, as well as their susceptibility to climatic variations, insect pests, and other variables. Consequently, the availability of these resources is limited, hence highlighting the increasing significance of chemical fibers as primary textile raw materials. This study primarily examines the recycling and treatment methods for polyester/viscose fiber, whereas the essential constituents of viscose fiber and cotton are the same. Notably, China has the position of the largest producer of viscose, with its production capacity for viscose staple fiber accounting for 73% of the global total production in 2021. To fulfill the objective of obtaining high-value pyrolysis products from waste textile fibers, an inexpensive clay catalyst, namely MMT, was employed. This study involves the synthesis of a set of cost-effective tungsten-manganese bimetallic supported MMT catalysts using the equal volume wet impregnation method. The catalytic performance of several catalysts in the hydrodeoxidation process of polyester/viscose fibers was evaluated and enhanced, with the aim of investigating an improved catalytic approach for the pyrolysis of textile fibers.

Materials and methods

Material

Previous research has indicated that the optimal pyrolysis synergistic effect was observed when polyester and viscose fibers were combined in a mass ratio of 1:2 (abbreviated as P1V2) [25]. Hence, our study delved deeper into the catalytic

pyrolysis characteristics of P1V2. The MMT powder (K10) utilized in the experiment was purchased from Qianyan Chemical Technology Co., Ltd. (Wuhan, China), the composition of MMT was shown in Fig. S1. The chemical $Na_2WO_4{\cdot}2H_2O$ (analytically pure) and $Mn(NO_3)_2$ solution with a concentration of 50 wt% were supplied by Chengdu Kelon Chemical Reagent Factory (China).

Preparation of catalyst

Metal supported MMTs were synthesized using the equal volume wet impregnation process. To conduct a comparative analysis of the catalytic activity, tungsten or manganese monometallic supported catalysts were also synthesized alongside tungsten-manganese bimetal supported catalysts. The monometallic loading of MMT was conducted using the following procedure: the designated reagent was dissolved in deionized water, and subsequently, the MMT was submerged in the solution at ambient temperature. The mixture was agitated for a duration of 1 h, followed by a 24-h period of air drying. Finally, the sample was subjected to oven drying at a temperature of 100 °C for a duration of 4 h. Subsequently, the catalyst underwent calcination in a Muffle furnace at a temperature of 550 °C and was subsequently activated for a duration of 4 h. This process resulted in the production of a catalyst supported by mono-metal MMT.

The procedure for loading tungsten-manganese bimetal onto montmorillonite (MMT) involved the following steps: first, an aqueous solution containing a specific concentration of manganese nitrate was made in accordance with the metal loading's quality standards, and then the manganese nitrate was loaded onto the surface of montmorillonite. It was stirred for 1 h, then left to stand for a full day before being dried in the shade. Following 4 h of drying at 100 °C in the oven, the catalyst intermediate was produced; Create a certain concentration of aqueous sodium tungstate solution, apply it to the catalyst intermediate's surface, agitate for 1 h, and then let it stand for 24 h. After that, dry it in the shade, dry it in an oven at 100 °C for 4 h, then calcine it at 550 °C in a muffle furnace. Obtain new MMT catalyst loaded with tungsten manganese bimetallic after 4 h of activation. The catalysts prepared are all powders and were screened with a 100 mesh sieve before use.

Catalyst characterization

The specific surface areas and porous structures (mean pore diameters and pore volumes) of the different catalysts were measured using a Belsorp Max II instrument (USA) at an operating temperature of -196 °C for N_2 adsorption and desorption. All catalysts had their Brunauer–Emmett–Teller (BET) specific surface area measured using a multi-point method in the relative pressure range of 0.05–0.35. The thermodynamic Barrett-Joyner-Helenda (BJH) method was used to calculate the pore size based on the adsorption and desorption branches of the isotherms. To determine the catalysts' total pore volumes, a relative pressure of 0.99 was chosen.

The acidities of the catalysts were determined using temperature programmed desorption of NH_3 (NH_3-TPD) studies (AMI-300, Altamira Instruments, USA). The

samples' actual metal loading contents were measured using the Agilent 5100 inductively coupled plasma-optical emission spectrometer (ICP-OES), and the results are illustrated in Table S1. X-ray diffraction (XRD) equipped with a Cu Kα radiation was used to determine the crystal structures of the catalysts using a Rigaku Ultima IV diffractometer (Japan). The X-ray tube operated at 40 kV and 40 mA, with a scan range of 5° to 90° (2θ) and a speed of 5°/min. The XRD patterns are shown in Fig.S1. The Thermo Scientific ESCALAB Xi + X-ray photoelectron spectrometer (XPS) was used to determine the state of metal oxides in metal-supported catalysts.

Pyrolysis–gas chromatography/mass spectrometry (Py-GC/MS) experiment

Pyrolysis analysis (Py) experiments were conducted on the Pyroprobe 5200 (CDS Analytical, USA). High purity helium gas (99.999%) was used to purge the volatiles generated during pyrolysis through a transport pipeline to a gas chromatograph (GC) (GC-450, Varian, USA) equipped with an online mass spectrometer (MS) (240-MS, Varian, USA) for analysis. The parameter setups and operational techniques of the pyrolysis experiments were detailed in our previous article [26].

Results and discussion

Catalytic pyrolysis of tungsten-manganese bimetallic supported MMT with different contents

Performance analysis of catalysts

All catalysts exhibited the distinctive MMT peaks in the XRD patterns (Fig.S1) at $2\theta = 22°$, suggesting that metals loading had no effect on the MMT skeleton. On bimetallic loaded MMT, the characteristic diffraction peaks of WO_3 and MnO_2 with approximately $2\theta = 35.5°$, 56° were observed, respectively [27, 28]. The composition of the pyrolysis oil is primarily influenced by the pore size and acidity of the catalyst [29]. Research has identified a positive association between the concentration of acid sites and the capacity to perform deoxygenation and aromatization processes [30]. The investigation of metal-supported catalysts revealed that the metal support layer had the ability to control the pore size structure of the carrier material. Furthermore, it was observed that the presence of mesopores in the catalyst contributes positively to enhancing the selectivity of aromatic hydrocarbons [31]. The N_2 adsorption and desorption isotherms of tungsten-manganese bimetallic loadings of 5 wt%, 10 wt%, 15 wt%, and 20 wt% with a constant tungsten-manganese loading ratio of 1:1 are shown in Fig. 1, while Table 1 shows the abbreviations and structural parameters of these catalysts.

The specific surface area, pore volume, and average pore diameter of the unloaded metal MMT were observed to be 262.46 m^2/g, 1.265 cm^3/g, and 14.18 nm, as indicated in Table 1. Bimetallic loading dramatically decreased the specific surface area when compared to untreated MMT. This is because metal elements stick

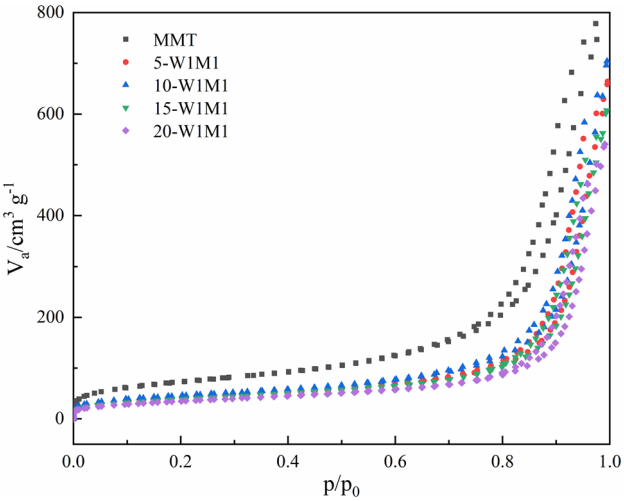

Fig. 1 N_2 adsorption and desorption isotherms of tungsten-manganese bimetallic loading at 5 wt%, 10 wt%, 15 wt%, and 20 wt%

Table 1 Structural parameters of catalysts with different bimetallic loads

Bimetallic content	Catalyst abbreviation	S_{BET} (m^2/g)[a]	Pore volume			Average aperture (nm)[d]
			V_{total} (cm^3/g)[b]	V_{micro} (cm^3/g)[c]	V_{meso} (cm^3/g)[c]	
0	MMT	262.46	1.265	0.17546	1.090	14.18
5 wt%	5-W1M1	149.19	0.965	0.00863	0.956	21.54
10 wt%	10-W1M1	165.45	1.028	0.00556	1.022	20.7
15 wt%	15-W1M1	142.16	0.899	0.07205	0.827	20.08
20 wt%	20-W1M1	128.5	0.829	0.01941	0.810	19.91

[a]By Multi-point BET method. [b]By total pore volume at $P/P_0 = 0.99$. [c]By t-plot method. [d]By BJH method

to the MMT's interior pore channels and surfaces during metal loading. The creation of new mesoporous structures caused by metal loading can be used to explain why the average pore width of the MMT loaded with tungsten-manganese increased after the metals were loaded. The obtained outcome exhibits resemblance to the experimental findings reported by Fang et al. [32], which showed that the introduction of metal Fe into the catalyst led to an increase in the average pore width. This phenomenon can be attributed to the development of comparable novel mesoporous structures on the surface of the catalyst. The catalyst containing a 10 wt% loading of tungsten-manganese bimetal (10-W1M1) exhibited the greatest specific surface area and pore volume, measuring 165.45 m^2/g and 1.028 cm^3/g. As the loading climbed to 15 wt% and 20 wt%, there was a corresponding drop in both specific surface area and pore volume. This observation suggests a rise in the loading capacity of the

Table 2 Acid amount of catalyst and content of different acid sites

Catalyst	Acid amount[a] (umol/g)	Acid sites content (%)[a]		
		Weak	Medium	Strong
MMT	296.14	16.2	26.6	57.2
5-W1M1	468.83	24.2	26.2	49.6
10-W1M1	552.47	27.5	22.2	50.3
15-W1M1	532.36	23.7	28.1	48.1
20-W1M1	506.31	37.4	18.4	44.2

[a]The number of acid sites was normalized integration values

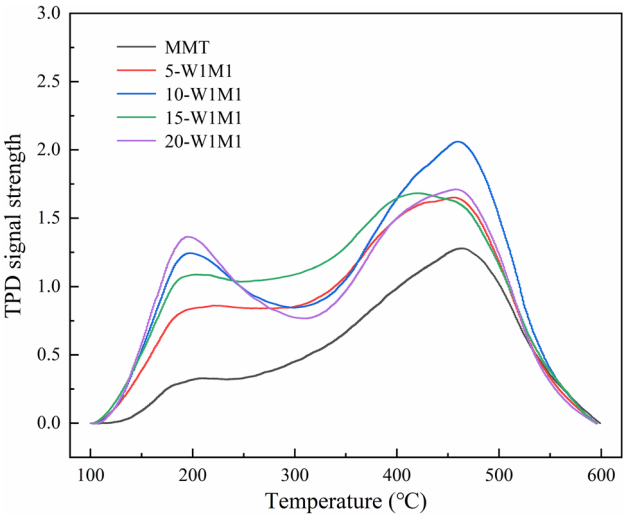

Fig. 2 NH_3-TPD spectra of MMT catalysts modified with different contents (5 wt%, 10 wt%, 15 wt%, and 20 wt%) of tungsten-manganese bimetal

catalyst, accompanied by the agglomeration of catalyst particles and subsequent blockage of certain pore channels. The bimetal concentration rose to 15 wt% and 20 wt%, and the micropore volume increased, which also indicated the aggregation phenomena that prevented tungsten-manganese dispersion into the pores. As depicted in Fig. 1, the catalysts that underwent modification exhibited a preserved IV type N_2 adsorption–desorption isothermal curve. This observation suggests that the catalysts continued to be predominantly characterized by a mesoporous structure [33]. The results of BET showed that metal ions were successfully dispersed on the surface of MMT and adjust the aperture. Generally speaking, it can be stated that mesoporous catalysts possessing greater pore size and suitable specific surface area have the capability to create favorable conditions for the process of late catalytic pyrolysis of biobased macromolecules [34].

To conduct a more comprehensive analysis of alterations in acidity, the quantities of acid and site content were measured and are presented in Table 2. Figure 2 shows

the NH_3-TPD spectra of these catalysts. Significant alterations in the distribution of acid sites were observed while varying the quantity of tungsten-manganese bimetal. The alteration in acidity of the catalyst can be attributed to the presence of acidic sites on the external surface or channels of the catalyst, as well as the interaction between metal species and proton acids or other functional groups [33, 34]. Based on the data presented in Table 2, the measured concentration of acid in MMT was determined to be 296.14 umol/g. The distribution of acid within MMT was found to consist of weak acid, medium strong acid, and strong acid, accounting for 16.2%, 26.6%, and 57.2% of the total acid content. The catalytic activity of MMTs for deoxidation and cracking of textile fibers was found to be poor, perhaps because to their mild acidity. However, it was observed that mesoporous catalysts did not quickly get deactivated as a result of coking [35, 36]. Following the loading of tungsten-manganese bimetal, there was an observed increase in the proportion of weak acid, accompanied by a decrease in the proportion of strong acid. This suggests that the interaction between the metal and protic acid resulted in the transformation of strong acid into medium or weak acid. Furthermore, the introduction of bimetal to the catalyst resulted in an increase in particle size, a decrease in dispersibility, a reduction in the coverage of acid sites, and the formation of additional acid sites due to the presence of metals. Consequently, there was a substantial increase in the overall acidity.

Based on the aforementioned findings, it is evident that the MMT mesoporous molecular sieve lacking metal loading exhibited bigger pore diameters and greater rates of molecular diffusion, hence demonstrating superior resistance to coking compared to microporous molecular sieves. Nevertheless, the catalytic activity of mesoporous molecular sieves was poor as a result of the insufficient presence of efficient acid sites [37]. Following the modification of MMT with tungsten-manganese bimetal, certain effects were observed. The presence of the bimetal led to the undesirable consequences of pore blockage and a reduction in the overall surface area of the catalyst, both of which had a negative impact on its catalytic activity. However, it was also observed that the acidity of the MMT catalyst was initially low, but increased after the modification with tungsten-manganese bimetal. Consequently, it was anticipated that the inclusion of bimetal would yield novel active sites, thereby resulting in an increased quantity of active sites involved in the deoxygenation reaction. This augmentation in active sites could potentially counterbalance the decline in activity stemming from the reduction in surface area.

Effect of tungsten-manganese bimetallic loading on catalytic pyrolysis of textile fibers

In order to study the effect of tungsten-manganese supported MMT on the catalytic pyrolysis of P1V2, MMT catalysts with different tungsten-manganese content (5-W1M1, 10-W1M1, 15-W1M1, 20-W1M1) were synthesized. The supported ratio of tungsten to manganese was 1:1, while the ratio of sample P1V2 to catalyst was 1:4. To enhance comprehension of the impact of various supporting metal catalysts on the allocation of pyrolysis products, the aforementioned compounds were classified into eight distinct categories based on the functional structure of pyrolysis products: monocyclic aromatic hydrocarbons (MAHs), polycyclic aromatic hydrocarbons

Table 3 Main pyrolysis compounds of P1V2 catalyzed by bimetal supported MMT with different content

Compound	Peak area/%				
	MMT	5-W1M1	10-W1M1	15-W1M1	20-W1M1
MAHs	24.02	35.98	40.38	39.10	34.32
PAHs	34.23	32.36	32.72	31.56	37.96
Other light hydrocarbons	3.84	3.89	3.43	4.44	3.66
Phenols and alcohols	8.27	9.91	8.77	8.90	9.09
Acids and esters	16.32	7.29	4.49	5.77	4.84
Aldehydes and ketones	7.49	1.89	2.34	1.87	3.23
Furans	6.52	7.47	6.75	7.16	6.35
Other oxygenated compounds	0.30	1.21	1.12	1.19	0.54

Table 4 Main pyrolysis compounds of P1V2 catalyzed by tungsten and manganese supported MMT

Compound	Peak area/%			
	Tungsten -5%	Tungsten -10%	Manganese -5%	Manganese -10%
MAHs	23.95	21.46	29.98	26.51
PAHs	44.90	49.14	42.88	49.56
Other light hydrocarbons	4.83	4.43	2.45	3.71
Phenols and alcohols	9.97	9.99	6.89	8.21
Acids and esters	5.33	5.13	6.87	3.89
Aldehydes and ketones	1.89	2.26	5.10	0.61
Furans	8.72	7.46	5.56	7.32
Other oxygenated compounds	0.40	0.14	0.27	0.19

(PAHs), other light hydrocarbons, phenols and alcohols, acids and esters, aldehydes and ketones, furans and other oxygenated compounds. The distribution results of corresponding pyrolysis products are shown in Table 3 and Fig.S2. Table 4 presents the distribution of pyrolysis products during the catalytic cracking of P1V2 with tungsten and manganese single metal supported MMT, for the purpose of comparison with bimetallic materials.

All MMT catalysts assisted by tungsten-manganese bimetal greatly decreased the proportion of compounds containing oxygen when compared to MMT, dropping from 37.91% to 27.77%, 23.47%, 24.89%, 24.05% of 5-W1M1, 10-W1M1, 15-W1M1, 20-W1M1. In the absence of tungsten-manganese bimetal, the contents of acids and esters, aldehydes and ketones in the pyrolysis products catalyzed by MMT were 16.32% and 7.49%, respectively. After supported bimetal, the contents of acids and esters, aldehydes and ketones were significantly reduced. When the load of tungsten-manganese bimetal was 10 wt%, the contents of acids and esters, aldehydes and ketones were reduced to 4.49% and 2.34%. Hence, the utilization of a tungsten-manganese bimetal supported MMT catalyst demonstrates a notable

capability in efficiently facilitating the deoxygenation and decarboxylation processes of pyrolysis steam, which will greatly enhance the quality and stability of the bio-oil.

The results presented in Table 4 demonstrate that the MMT catalysts supported with tungsten and manganese single metals exhibited noteworthy deoxidation effects. Catalysts participate in the deoxygenation of highly oxygenated compounds to different types of hydrocarbons through deoxygenation pathways such as aldol condensation, decarboxylation, decarbonylation, dehydration and Diels – Alder reactions [37, 38]. Compared with MMTs containing individual metals such as tungsten and manganese, the incorporation of tungsten-manganese bimetallic species into MMT catalysts yielded notable effects on the resulting pyrolysis products. Specifically, the utilization of tungsten-manganese bimetallic loaded MMT catalysts led to a greater production of MAHs. Bimetallic catalysts exhibit considerable promise owing to the synergistic interplay between their acidity and redox characteristics, resulting in enhanced selectivity and stability of the resultant products [39, 40]. In this study, tungsten-manganese bimetallic supported MMT significantly enhanced the selectivity of MAHs, which also confirmed the advantages of bimetallic catalysts in catalytic pyrolysis. In comparison to single metal catalysts composed of tungsten or manganese, bimetallic catalysts consisting of tungsten and manganese demonstrated superior skills in achieving equilibrium of MAHs and PAHs. This characteristic renders them more desirable for the composition of bio-oil intended for potential use as transport fuels [41]. The bimetal active site's synergistic action not only enhances the deoxidation effect of the bimetal catalyst due to their higher aromatics selectivity (MAHs and PAHs), but also reduces PAHs selectivity, preventing active site deactivation and improving catalyst stability [40, 42].

The selectivity of 5-W1M1, 10-W1M1, 15-W1M1 and 20-W1M1 to aromatics (MAHs and PAHs) was 68.34%, 73.10%, 70.66% and 72.28%, that is, the sequence of catalytic effects on aromatics was as follows: 10-W1M1 > 20-W1M1 > 15-W1 M1 > 5-W1M1, which was the result of tungsten-manganese bimetal converting oxygen-containing substances into hydrocarbon compounds, bimetal can promote the Diels–Alder reaction and the deoxidation of oxygen-containing aromatic compounds, thereby increasing the yield of aromatic compounds. Under catalytic pyrolysis conditions, MMT with a tungsten-manganese loading of 10 wt% had the highest aromatics yield of 73.10%, with MAHs of 40.38%, which may be attributed to two factors: On the one hand, higher surface area and pore volume increased the accessibility of the pyrolysis active center; on the other hand, higher acidity increased the number of active sites in the catalytic reaction, and more oxygen-containing compounds were converted to aromatics via acid catalyzed deoxidation, cleavage, and aromatization[28, 32]. The catalytic performance of 5-W1M1 was unsatisfactory, possibly due to its low acidity and inadequate provision of active sites, resulting in insufficient deoxidation. The micropore volume of 15-W1M1 (0.07205 cm^3/g) was significantly greater than that of 20-W1M1 (0.01941 cm^3/g). This disparity in micropore volume resulted in a larger amount of oxygen-containing compounds being unable to facilitate the conversion process. Consequently, this had a negative impact on the yield of aromatics. As a result, the selectivity of 20-W1M1 towards aromatics was higher than that of 15-W1M1. When the tungsten-manganese loading was 15 wt% and 20 wt%, the MAHs yield was significantly reduced to 34.32%, that

is, the catalyst with higher metal loading promoted the formation of more PAHs, which may be due to the high tungsten-manganese loading resulting in a large loss of specific surface area and acid content [43]. Without a doubt, the loading of catalysts plays a pivotal role in both the production and quality of bio-oil. A higher quantity of catalysts promotes secondary reactions and influences the development of tar, ultimately leading to a decrease in the yield of bio-oil [43, 44].

The findings of this study suggest that a moderate loading of tungsten-manganese can enhance the production of MAHs, but an excessive loading of tungsten-manganese can readily increase the formation of PAHs. PAHs are known to possess hazardous and carcinogenic properties. Therefore, it is imperative to exercise stringent control over the generation and accumulation of these chemical components during the pyrolysis process. The accumulation of coke, resulting from the polymerization of oxygen-containing intermediates, often occurs on the catalyst's external surface. In contrast, catalytic coke mostly forms from polycyclic aromatic hydrocarbons (PAHs) and is deposited within the catalyst channel [22]. In brief, the incorporation of tungsten and manganese elements into the MMT carrier resulted in an increased efficacy in eliminating oxygen-containing compounds and promoting the formation of hydrocarbons in the bio-oil. This notable deoxidation and selective aromatization can be attributed to the balanced presence of Lewis and Brønsted acid sites within the catalyst, as well as the heightened hydrogen transfer reaction that occurs during pyrolysis [45]. The largest yield of MAHs and the lowest yield of PAHs were observed when the tungsten-manganese bimetallic load was 10 wt%, specifically referred to as 10-W1M1. Hence, it is deemed appropriate to conduct a more comprehensive investigation into the impact of varying tungsten manganese ratios on the distribution of P1V2 catalytic products, given a tungsten-manganese bimetallic loading of 10 wt%.

Table 5 Structural parameters of catalyst with bimetallic loading ratio

Tungsten manganese ratio	Catalyst abbreviation	S_{BET} (m^2/g)[a]	Pore volume			Average aperture (nm)[d]
			V_{total} (cm^3/g)[b]	V_{micro} (cm^3/g)[c]	V_{meso} (cm^3/g)[c]	
4:1	10-W4M1	145.56	1.169	0.00817	1.161	25.63
2:1	10-W2M1	163.59	1.175	0.00788	1.167	22.23
1:1	10-W1M1	165.45	1.028	0.00556	1.022	20.70
1:2	10-W1M2	175.28	1.171	0.00561	1.165	20.01
1:4	10-W1M4	177.32	1.106	0.00520	1.101	19.66

[a]By Multi-point BET method. [b] By total pore volume at $P/P_0 = 0.99$. [c]By t-plot method. [d]By BJH method

Effect of tungsten-manganese bimetal loading ratio on pyrolysis performance

Performance analysis of catalysts

Table 5 presents the structural features of MMT catalysts supported by various tungsten-manganese ratios, with a tungsten-manganese bimetallic load of 10 wt%. In comparison to MMT, the introduction of varying tungsten-manganese bimetallic ratios on MMT exhibits a similar effect in reducing the BET surface area and total pore volume. With the decrease of tungsten metal loading and the increase of manganese metal loading, the specific surface area of the catalyst increased from 145.56 m^2/g to 177.32 m^2/g, and the average pore diameter decreased from 25.63 nm to 19.66 nm, indicating that manganese is more likely to enter the channels of MMT than tungsten.

Figure 3 shows the NH_3-TPD spectra of MMT catalysts modified with different tungsten-manganese ratios. Table S2 shows the details of the total acid content and the content of different acid sites of the catalysts with five different bimetal loading ratios. The process of deoxidizing bio-oil is primarily achieved by a dehydration reaction facilitated by an acid catalyst. The effectiveness of this catalyst in deoxidizing bio-oil can be enhanced by using a transition bimetal in an optimal ratio. Metal ions can be dispersed on the internal and external surfaces of the MMT catalyst, or they can be introduced as compensating cations in the MMT structure [46]. The introduction of various tungsten-manganese bimetal ratios into MMT catalysts resulted in a notable alteration in the overall acid content. Specifically, there was an increase in acid levels as a consequence of the interaction between the metal species and proton sites located within the catalytic channel or on its surface. When the tungsten-manganese load ratio was 1:1 (10-W1M1), the acid content reached the

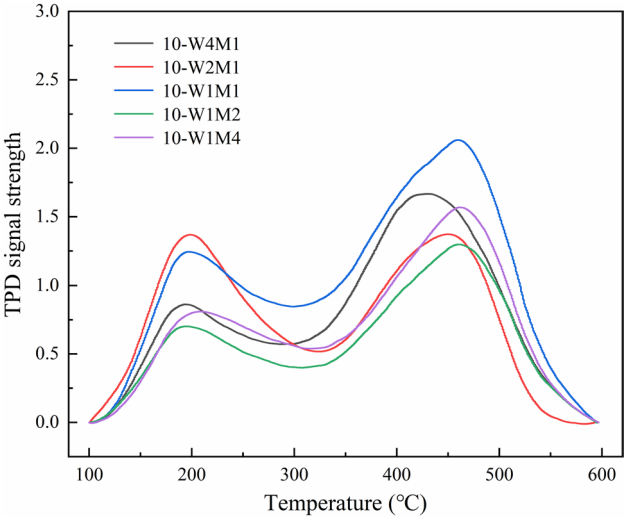

Fig. 3 NH_3-TPD spectra of MMT catalyst modified by tungsten-manganese ratio (4:1, 2:1,1:1,1:2, and 1:4)

highest value (552.37 umol/g). More acidic sites are beneficial for deoxygenation reactions, thus more conducive to the formation of aromatic hydrocarbons, this is because strong acids and higher overall acidity stimulate catalyst hydrogenation and deoxidation, resulting in higher MAHs yields. However, polymerization processes are more likely to occur at strong acid sites, producing more PAHs. Therefore, the distribution of strong and weak acids in the catalyst impacts the selectivity of MAHs and PAHs [47]. Furthermore, achieving increased deoxidation and minimizing charring necessitates the careful management of the quantity and nature of acid sites present in the catalyst [41]. Additionally, the acidity balance of MMT is enhanced through the application of varying quantities of tungsten-manganese bimetal loading.

To determine the status of metal oxides in metal supported catalysts, XPS analysis was performed. The states of manganese oxide and tungsten oxide might be distinguished using the spectral properties of W 4f, Mn 2p. Figure 4 shows the W 4f, Mn 2p spectra curves of the fresh and spent catalyst. Peaks centered at 35.02 and 642.17 eV were seen in the fresh 10-W1M1. These values corresponded to the features of W^{6+} and Mn^{4+}, confirming the presence of WO_3 and MnO_2 in the catalyst. In the XPS spectrum of spent catalyst, the central binding energy of W increased slightly from 35.02 to 35.28 eV, and the density of electron cloud around W metal decreased, whereas the band of Mn widened and moved slightly toward the direction of low binding energy, and the density of electron cloud around Mn metal increased.

Effect of tungsten-manganese bimetallic loading ratio on catalytic pyrolysis

To clarify the effect of different tungsten-manganese bimetallic modifications of MMT on the formation of pyrolysis products, CFP tests were performed on P1V2 at 700 °C on different catalysts, namely 10-W4M1, 10-W2M1, 10-W1M1, 10-W1M2 and 10-W1M4. The ratio of P1V2 to catalyst was maintained at 1:4. Table S3 and Fig. 5 show the product distribution of P1V2 catalytic pyrolysis using tungsten-manganese bimetallic supported MMT catalyst. In the scenario where the tungsten-manganese concentration remains constant at 10 wt%, alterations in the

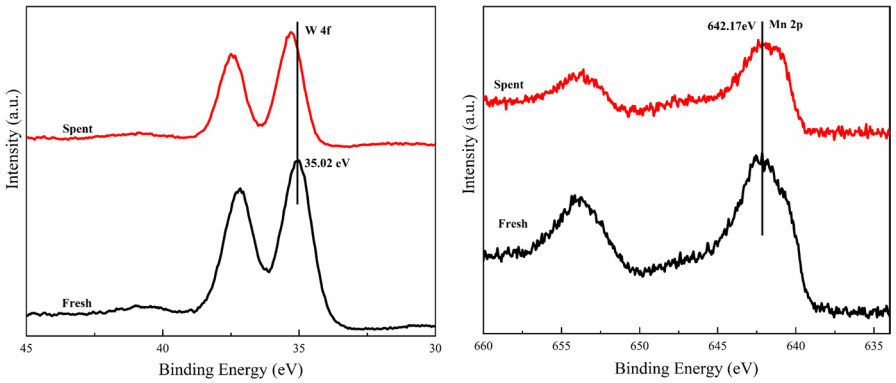

Fig. 4 The tungsten (W) and manganese (Mn) XPS spectra of fresh and spent catalyst (10-W1M1)

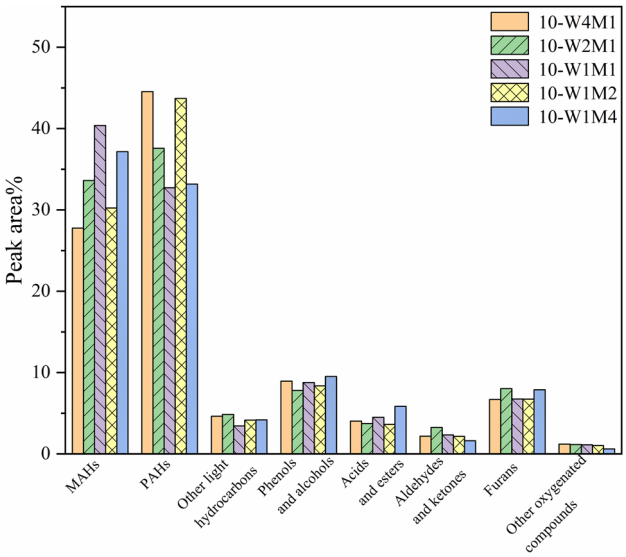

Fig. 5 Relative contents of P1V2 catalytic pyrolysis products by MMT supported on different tungsten-manganese ratio (4:1, 2:1,1:1,1:2, and 1:4) at 700 °C

tungsten-manganese ratio would have a substantial impact on the production yield of pyrolysis products such as MAHs, PAHs and oxygenated compounds. The data shown in Table S3 demonstrates that aromatic hydrocarbons, specifically MAHs and PAHs, were the predominant outcomes. This indicates that MMT catalysts, when modified with varying proportions of bimetallic compounds, can effectively facilitate the manufacture of aromatic compounds with selectivity. The catalyst exhibits a notable degree of selectivity towards aromatic hydrocarbons, maybe attributed to the interaction between the active metal and the carrier MMT. This interaction is believed to induce structural modifications at the corresponding active acid site. Ultimately, the combined catalytic action of the two metals leads to a modification in the preferential formation of products. It has been substantiated through empirical research that metals employed as acid catalysts can effectively facilitate decarboxylation and decarbonization reactions, thus augmenting the overall production of hydrocarbons [48]. Various metal loading ratios displayed distinct variations in pyrolysis products, potentially attributable to their inherent acidity and mesoporous structure.

Compared with MMT, 10-W4M1, 10-W2M1, 10-W1M1, 10-W1M2 and 10-W1M4 could significantly promote the production of MAHs, and the yields were 27.77%, 33.61%, 40.38%, 30.24% and 37.16%. Therefore, the physicochemical features of the catalysts were altered by varying the tungsten-manganese bimetallic ratios, resulting in distinct catalytic activity seen in the CFP process. By comparing the distribution of P1V2 pyrolysis products using these five different catalysts, it can be observed that higher amounts of MAHs and lower amounts of PAHs tend to be produced when the tungstan-manganese load ratio was 1:1. The PAHs yield

of 10-W1M1 catalyst was the lowest (32.72%), while the PAHs yield of 10-W4M1 catalytic pyrolysis was the highest (44.54%). The low PAHs yield will help suppress the formation of coke, thereby reducing catalyst deactivation [49]. The superior deoxidation performance of the 10-W1M1 catalyst in the production of MAHs in bio-oil samples can be ascribed to its suitable pore structure and the well-balanced arrangement of Lewis acid and Brønsted acid sites inside the pores.

The quantification of the aromatics yield was demonstrated in Fig. 6. Benzene was found to be the predominant constituent among all aromatic compounds in the category of MAHs, while biphenyls were identified as the most prevalent constituents among PAHs. The observation in Fig. 6 reveals that catalysts with varying bimetallic loading ratios also yield competitive levels of MAHs and PAHs. The study revealed that altering the loading ratio of tungsten-manganese metal during the pyrolysis process resulted in the preferential generation of distinct hydrocarbon compounds within the bio-oil samples. Compared with MMT, 10-W1M2 and 10-W4M1 significantly inhibited the formation of MAHs and promoted the increase of PAHs. As can be seen from Table S4, when using a tungsten-manganese bimetallic ratio of 1:1, that is, 10-W1M1, MAHs significantly increased, while PAHs decreased. The relative content of benzene in aromatic hydrocarbons can reach 40.75%, much higher than 29.32% of MMT. The observed phenomenon could perhaps be attributed to the influence of the tungsten-manganese bimetal on the catalytic hydrogenation capacity of the catalyst, hence facilitating the dealkylation process of xylene, toluene, and other aromatic compounds. According to literature report, bimetallic modified catalysts can inhibit the generation of

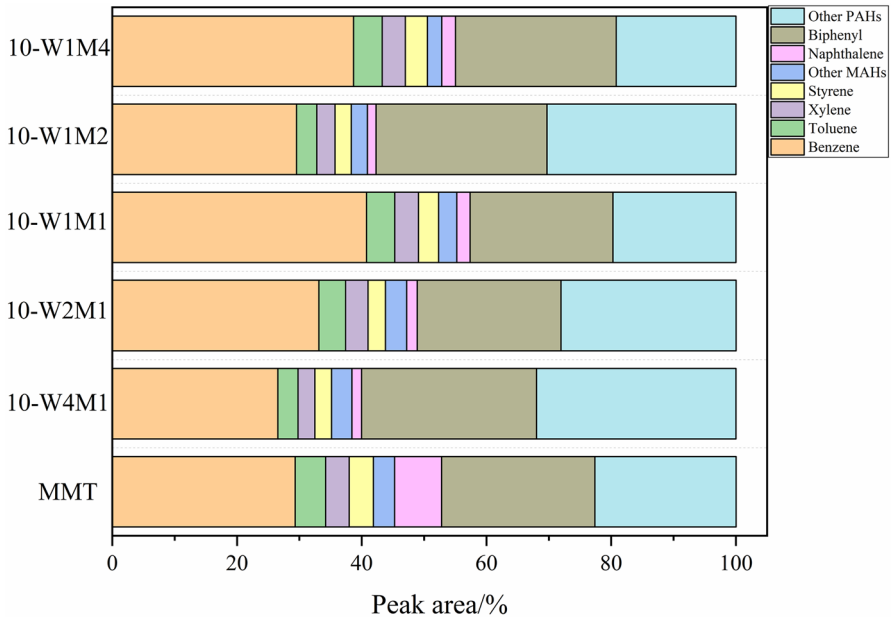

Fig. 6 The aromatic hydrocarbon selectivity from the pyrolysis of P1V2 by MMT supported on different tungsten-manganese ratio (4:1, 2:1,1:1,1:2, and 1:4)

MAHs due to their optimized acidity and enhanced hydrogen transfer ability [50]. This is consistent with Table S2, where 10-W1M1 exhibited the strongest acidity. A significant synergistic effect was seen at a tungsten-manganese ratio of 1:1 (10-W1M1), resulting in a substantial enhancement of the catalyst's regulatory efficacy towards MAHs and PAHs. Hence, it can be observed that the utilization of a 1:1 ratio of tungsten to manganese in the bimetallic system resulted in a heightened level of synergy, thereby enhancing the generation of beneficial MAHs.

Conclusions

This research presents a demonstration of the superior bio-oil deoxidation activity exhibited by a tungsten-manganese bimetal-supported MMT catalyst during the pyrolysis of textile fibers. The utilization of this catalyst significantly enhances the quality and stability of the resulting bio-oil. The bimetallic catalyst composed of tungsten and manganese exhibited enhanced deoxidation effectiveness and yielded a comparatively elevated concentration of aromatic hydrocarbons. The order of catalytic effect on aromatic hydrocarbons was 10-W1M1 > 20-W1M1 > 15-W1M1 > 5-W1M1. MMT with a bimetallic load of 10 wt% (10-W1M1) had the highest aromatics yield of 73.10%, with MAHs of 40.38%, due to its higher surface area and higher acidity. When the loading amounts were 15 wt% and 20 wt%, the yield of MAHs significantly decreased to 34.32%, indicating that the catalyst with higher metal loading promoted the formation of more PAHs. Compared with MMT, 10-W4M1, 10-W2M1, 10-W1M1, 10-W1M2 and 10-W1M4 could significantly promote the production of MAHs, and the yields were 27.77%, 33.61%, 40.38%, 30.24% and 37.16%. The superior deoxidation performance of the 10-W1M1 catalyst in the production of MAHs in bio-oil samples can be ascribed to its well-suited pore structure and the equitable allocation of Lewis acid and Brønsted acid sites within the pores. The variation in outcomes observed across different catalyst types can be attributed to the distinct physical and chemical features resulting from the loading of tungsten-manganese bimetallic compounds. Furthermore, the acid balance and mesoporous structure of catalysts exert an influence on the activity and selectivity of these catalysts.

Supplementary Information The online version contains supplementary material available at https://doi.org/10.1007/s11144-024-02666-2.

Acknowledgements This work was financially supported by the National Natural Science Foundation of China [No. 51721091].

Data availability The authors confirm that the data supporting the findings of this study are available within the article or its supplementary materials.

Declarations

Competing Interest The authors declare no conflicts of interest regarding this article.

References

1. Haslinger S, Hummel M, Anghelescu-Hakala A, Määttänen M, Sixta H (2019) Upcycling of cotton polyester blended textile waste to new man-made cellulose fibers. Waste Manag 97:88–96. https://doi.org/10.1016/j.wasman.2019.07.040
2. Li X, Wang L, Ding X (2021) Textile supply chain waste management in China. J Clean Prod 289:125147. https://doi.org/10.1016/j.jclepro.2020.125147
3. Xia G, Han W, Xu Z, Zhang J, Kong F, Zhang J, Zhang X, Jia F (2021) Complete recycling and valorization of waste textiles for value-added transparent films via an ionic liquid. J Environ Chem Eng 9:106182. https://doi.org/10.1016/j.jece.2021.106182
4. Mu B, Shao Y, McBride L, Hidalgo H, Yang Y (2023) Rapid fiber-to-fiber recycling of poly (ethylene terephthalate) and its dye from waste textiles without damaging their chemical structures. Resour Conserv Recycl 197:107102. https://doi.org/10.1016/j.resconrec.2023.107102
5. Loo SL, Yu E, Hu X (2023) Tackling critical challenges in textile circularity: a review on strategies for recycling cellulose and polyester from blended fabrics. J Environ Chem Eng 11:110482. https://doi.org/10.1016/j.jece.2023.110482
6. Sun C, Chen X, Zhuo Q, Zhou T (2018) Recycling and depolymerization of waste polyethylene terephthalate bottles by alcohol alkali hydrolysis. J Cent South Univ 25:543–549. https://doi.org/10.1007/s11771-018-3759-y
7. Wang Z, Burra KG, Lei T, Gupta AK (2021) Co-pyrolysis of waste plastic and solid biomass for synergistic production of biofuels and chemicals-A review. Prog Energy Combust Sci 84:100899. https://doi.org/10.1016/j.pecs.2020.100899
8. Rizal S, Olaiya FG, Saharudin NI et al (2021) Isolation of textile waste cellulose nanofibrillated fibre reinforced in polylactic acid-chitin biodegradable composite for green packaging application. Polymers (Basel) 13:1–15. https://doi.org/10.3390/polym13030325
9. Zhong X, Li R, Wang Z, Wang Y, Wang W, Yu D (2021) Highly flexible, transparent film prepared by upcycle of wasted jute fabrics with functional properties. Process Saf Environ Prot 146:718–725. https://doi.org/10.1016/j.psep.2020.12.013
10. Hanoğlu A, Çay A, Yanık J (2019) Production of biochars from textile fibres through torrefaction and their characterisation. Energy 166:664–673. https://doi.org/10.1016/j.energy.2018.10.123
11. Yu Z, Ahmad MS, Shen B, Li Y, Ibrahim M, Bokhari A, Klemeš JJ (2023) Activated waste cotton cellulose as renewable fuel and value-added chemicals: thermokinetic analysis, coupled pyrolysis with gas chromatography and mass spectrometry. Energy. https://doi.org/10.1016/j.energy.2023.128341
12. Gao X, Chang CR (2023) Preparing fuel-range chemicals via the direct and selective pyrolysis of disposable mask waste for sustainable environment. Catalysts. https://doi.org/10.3390/catal13040743
13. Lee HS, Jung S, Lin KYA, Kwon EE, Lee J (2023) Upcycling textile waste using pyrolysis process. Sci Total Environ 859:160393. https://doi.org/10.1016/j.scitotenv.2022.160393
14. Zhang H, Cheng YT, Vispute TP, Xiao R, Huber GW (2011) Catalytic conversion of biomass-derived feedstocks into olefins and aromatics with ZSM-5: the hydrogen to carbon effective ratio. Energy Environ Sci 4:2297–2307. https://doi.org/10.1039/c1ee01230d
15. Wang Y, Zeng Y, Fan L, Wu Q, Zhang L, Xiong J, Zhang J, Liao R, Cobb K, Liu Y, Ruan R, Wang Y (2023) Pyrolysis of different types of waste cooking oil in the presence/absence HZSM-5 catalyst: Influence of feedstock characteristics on aromatic formation. Fuel 351:128937. https://doi.org/10.1016/j.fuel.2023.128937
16. Yang H, Zhang J, Chen Z, Wan L, Li C, Zhang X, Li J, Tian R, Yu J, Gao S (2023) Base-acid relay catalytic upgrading of coal pyrolysis volatiles over CaO and HZSM-5 catalysts. J Anal Appl Pyrolysis 170:105926. https://doi.org/10.1016/j.jaap.2023.105926
17. Fan X, Wu Y, Tu R, Sun Y, Jiang E, Xu X (2020) Hydrodeoxygenation of guaiacol via rice husk char supported Ni based catalysts: the influence of char supports. Renew Energy 157:1035–1045. https://doi.org/10.1016/j.renene.2020.05.045
18. Santamaria L, Lopez G, Arregi A, Artetxe M, Amutio M, Bilbao J, Olazar M (2020) Catalytic steam reforming of biomass fast pyrolysis volatiles over Ni–Co bimetallic catalysts. J Ind Eng Chem 91:167–181. https://doi.org/10.1016/j.jiec.2020.07.050

19. Hong W, Zhang Y, Song J, Liu H, Zhang L, Wang H, Zhang Y, Jiang H (2023) Efficient preparation of phenol-enriched bio-oil using cobalt-modified montmorillonite K-10 catalyst. J Anal Appl Pyrolysis 170:105895. https://doi.org/10.1016/j.jaap.2023.105895
20. Balasundram V, Ibrahim N, Kasmani RM, Isha R, Hamid MKA, Hasbullah H, Ali RR (2018) Catalytic upgrading of sugarcane bagasse pyrolysis vapours over rare earth metal (Ce) loaded HZSM-5: effect of catalyst to biomass ratio on the organic compounds in pyrolysis oil. Appl Energy 220:787–799. https://doi.org/10.1016/j.apenergy.2018.03.141
21. Chen T, Yu J, Ma C, Bikane K, Sun L (2020) Catalytic performance and debromination of Fe–Ni bimetallic MCM-41 catalyst for the two-stage pyrolysis of waste computer casing plastic. Chemosphere 248:125964. https://doi.org/10.1016/j.chemosphere.2020.125964
22. Li Y, Nishu YD, Li C, Liu R (2022) Deactivation mechanism and regeneration effect of bi-metallic Fe-Ni/ZSM-5 catalyst during biomass catalytic pyrolysis. Fuel 312:122924. https://doi.org/10.1016/j.fuel.2021.122924
23. Miskolczi N, Ateş F, Borsodi N (2013) Comparison of real waste (MSW and MPW) pyrolysis in batch reactor over different catalysts. Part II: contaminants, char and pyrolysis oil properties. Bioresour Technol 144:370–379. https://doi.org/10.1016/j.biortech.2013.06.109
24. Balasundram V, Zaman KK, Ibrahim N, Kasmani RM, Isha R, Hamid MKA, Hasbullah H (2018) Catalytic upgrading of pyrolysis vapours over metal modified HZSM-5 via in-situ pyrolysis of sugarcane bagasse: effect of nickel to cerium ratio on HZSM-5. J Anal Appl Pyrolysis 134:309–325. https://doi.org/10.1016/j.jaap.2018.06.021
25. Peng H, Li P, Yang Q (2022) Investigation on the reaction kinetics, thermodynamics and synergistic effects in co-pyrolysis of polyester and viscose fibers. React Kinet Mech Catal 135:769–793. https://doi.org/10.1007/s11144-022-02167-0
26. Peng H, Li P, Yang Q (2022) Pyrolysis of polyester and viscose fiber over ZSM-5: synergistic effect and distribution of products. J Therm Anal Calorim 147:12535–12545. https://doi.org/10.1007/s10973-022-11521-2
27. Demir KÇ (2020) Corrosion behavior of electrodeposited Wo3 thin films. Ceram Int 46:4358–4364. https://doi.org/10.1016/j.ceramint.2019.10.159
28. Worku AK, Ayele DW, Habtu NG (2021) Influence of nickel doping on MnO2 nanoflowers as electrocatalyst for oxygen reduction reaction. SN Appl Sci. https://doi.org/10.1007/s42452-021-04746-7
29. Yildiz G, Ronsse F, Van DR, Prins W (2016) Challenges in the design and operation of processes for catalytic fast pyrolysis of woody biomass. Renew Sustain Energy Rev 57:1596–1610. https://doi.org/10.1016/j.rser.2015.12.202
30. Che Q, Yang M, Wang X, Yang Q, Rose Williams L, Yang H, Zou J, Zeng K, Zhu Y, Chen Y (2019) Influence of physicochemical properties of metal modified ZSM-5 catalyst on benzene, toluene and xylene production from biomass catalytic pyrolysis. Bioresour Technol 278:248–254. https://doi.org/10.1016/j.biortech.2019.01.081
31. Song W, Zhao C, Lercher JA (2013) Importance of size and distribution of Ni nanoparticles for the hydrodeoxygenation of microalgae oil. Chem - A Eur J 19:9833–9842. https://doi.org/10.1002/chem.201301005
32. Fang S, Shi C, Jiang L, Li P, Bai J, Chang C (2020) Influence of metal (Fe/Zn) modified ZSM-5 catalysts on product characteristics based on the bench-scale pyrolysis and Py-GC/MS of biomass. Int J Energy Res 44:5455–5467. https://doi.org/10.1002/er.5294
33. Wang X, Jin X, Wang H, Wang Y, Zuo L, Shen B, Yang J (2023) Catalytic pyrolysis of microalgal lipids to liquid biofuels: Metal oxide doped catalysts with hierarchically porous structure and their performance. Renew Energy 212:887–896. https://doi.org/10.1016/j.renene.2023.05.119
34. Zheng Y, Wang J, Liu C, Lu Y, Lin X, Li W, Zheng Z (2020) Efficient and stable Ni–Cu catalysts for ex situ catalytic pyrolysis vapor upgrading of oleic acid into hydrocarbon: Effect of catalyst support, process parameters and Ni-to-Cu mixed ratio. Renew Energy 154:797–812. https://doi.org/10.1016/j.renene.2020.03.058
35. Abdelsayed V, Smith MW, Shekhawat D (2015) Investigation of the stability of Zn-based HZSM-5 catalysts for methane dehydroaromatization. Appl Catal A Gen 505:365–374. https://doi.org/10.1016/j.apcata.2015.08.017
36. Wei Z, Chen L, Cao Q, Wen Z, Zhou Z, Xu Y, Zhu X (2017) Steamed Zn/ZSM-5 catalysts for improved methanol aromatization with high stability. Fuel Process Technol 162:66–77. https://doi.org/10.1016/j.fuproc.2017.03.026

37. Xue S, Luo Z, Wang W, Li S, Sun H, Zhou Q, Liang X (2020) Preparation of aromatics from catalytic pyrolysis of enzymatic lignin over double-layer metal supported core-shell catalyst. J Anal Appl Pyrolysis 150:104884. https://doi.org/10.1016/j.jaap.2020.104884
38. Solak A, Rutkowski P (2014) The effect of clay catalyst on the chemical composition of bio-oil obtained by co-pyrolysis of cellulose and polyethylene. Waste Manag 34:504–512. https://doi.org/10.1016/j.wasman.2013.10.036
39. Custodis VBF, Hemberger P, Ma Z, Van Bokhoven JA (2014) Mechanism of fast pyrolysis of lignin: Studying model compounds. J Phys Chem B 118:8524–8531. https://doi.org/10.1021/jp5036579
40. Gunawardena DA, Fernando SD (2018) Screening of transition metal/oxide-impregnated ZSM-5 catalysts for deoxygenation of biomass oxygenates via direct methane intervention. Biofuels 9:113–120. https://doi.org/10.1080/17597269.2016.1259523
41. Kumar R, Strezov V, Kan T, Weldekidan H, He J, Jahan S (2020) Investigating the effect of mono- and bimetallic/zeolite catalysts on hydrocarbon production during bio-oil upgrading from ex situ pyrolysis of biomass. Energy Fuels 34:389–400. https://doi.org/10.1021/acs.energyfuels.9b02724
42. Xue S, Luo Z, Zhou Q, Sun H, Du L (2021) Regulation mechanism of three key parameters on catalytic characterization of molybdenum modified bimetallic micro-mesoporous catalysts during catalytic fast pyrolysis of enzymatic hydrolysis lignin. Bioresour Technol 337:125396. https://doi.org/10.1016/j.biortech.2021.125396
43. Li K, Zhang G, Wang Z, Hu B, Lu Q (2020) Calcium formate assisted catalytic pyrolysis of pine for enhanced production of monocyclic aromatic hydrocarbons over bimetal-modified HZSM-5. Bioresour Technol 315:123805. https://doi.org/10.1016/j.biortech.2020.123805
44. Kumar R, Strezov V, Lovell E, Kan T, Weldekidan H, He J, Dastjerdi B, Scott J (2019) Bio-oil upgrading with catalytic pyrolysis of biomass using copper/zeolite-nickel/zeolite and copper-nickel/zeolite catalysts. Bioresour Technol 279:404–409. https://doi.org/10.1016/j.biortech.2019.01.067
45. Hernando H, Hernández-Giménez AM, Ochoa-Hernández C, Bruijnincx PCA, Houben K, Baldus M, Pizarro P, Coronado JM, Fermoso J, Čejka J, Weckhuysen BM, Serrano DP (2018) Engineering the acidity and accessibility of the zeolite ZSM-5 for efficient bio-oil upgrading in catalytic pyrolysis of lignocellulose. Green Chem 20:3499–3511. https://doi.org/10.1039/c8gc01722k
46. Hertzog J, Carré V, Jia L, Mackay CL, Pinard L, Dufour A, Mašek O, Aubriet F (2018) Catalytic fast pyrolysis of biomass over microporous and hierarchical zeolites: characterization of heavy products. ACS Sustain Chem Eng 6:4717–4728. https://doi.org/10.1021/acssuschemeng.7b03837
47. Yildiz G, Lathouwers T, Toraman HE, Van Geem KM, Marin GB, Ronsse F, Van Duren R, Kersten SRA, Prins W (2014) Catalytic fast pyrolysis of pine wood: effect of successive catalyst regeneration. Energy Fuels 28:4560–4572. https://doi.org/10.1021/ef500636c
48. Liu WJ, Li WW, Jiang H, Yu HQ (2017) Fates of chemical elements in biomass during its pyrolysis. Chem Rev 117:6367–6398. https://doi.org/10.1021/acs.chemrev.6b00647
49. Wu J, Chang G, Li X, Li J, Guo Q (2020) Effects of NaOH on the catalytic pyrolysis of lignin/HZSM-5 to prepare aromatic hydrocarbons. J Anal Appl Pyrolysis 146:104775. https://doi.org/10.1016/j.jaap.2020.104775
50. Lu Q, Wang Z, Guo H, Li K, Zhang Z, Cui M, Yang Y (2019) Selective preparation of monocyclic aromatic hydrocarbons from ex-situ catalytic fast pyrolysis of pine over Ti(SO4)2-Mo2N/HZSM-5 catalyst. Fuel 243:88–96. https://doi.org/10.1016/j.fuel.2019.01.102